Electronic Supplementary Information

Metal–Organic Framework-Derived Integrated Nanoarrays for Overall Water Splitting

Cao Guan, Haijun Wu, Weina Ren, Chunhai Yang, Ximeng Liu, Xiaofang Ouyang, Zeyi Song, Yuzhong Zhang, Stephen J. Pennycook, Chuanwei Cheng, John Wang

Supporting Figures

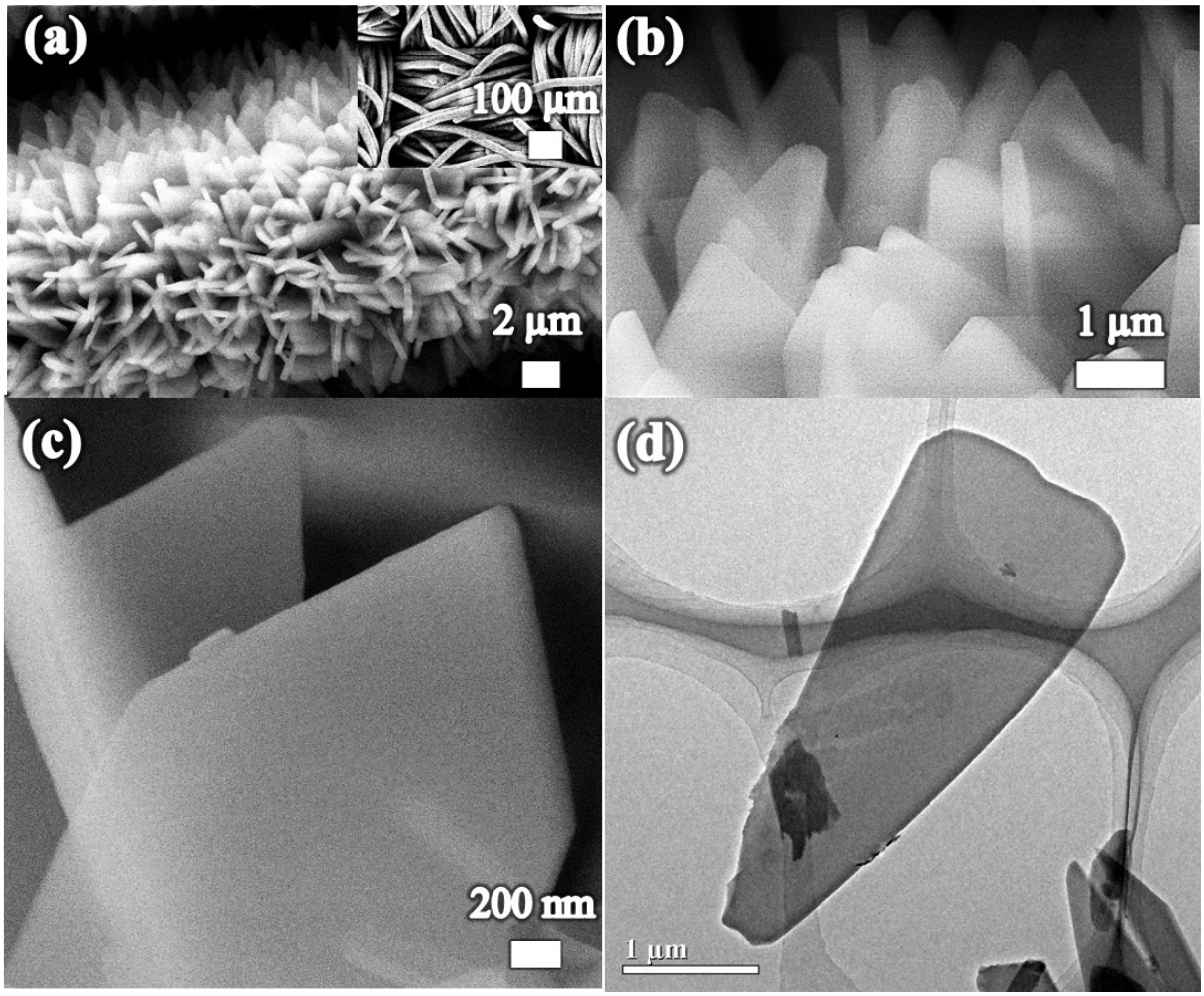

Figure S1. SEM (a-c) and TEM (d) images of Co-MOF. Related to Figure 1.

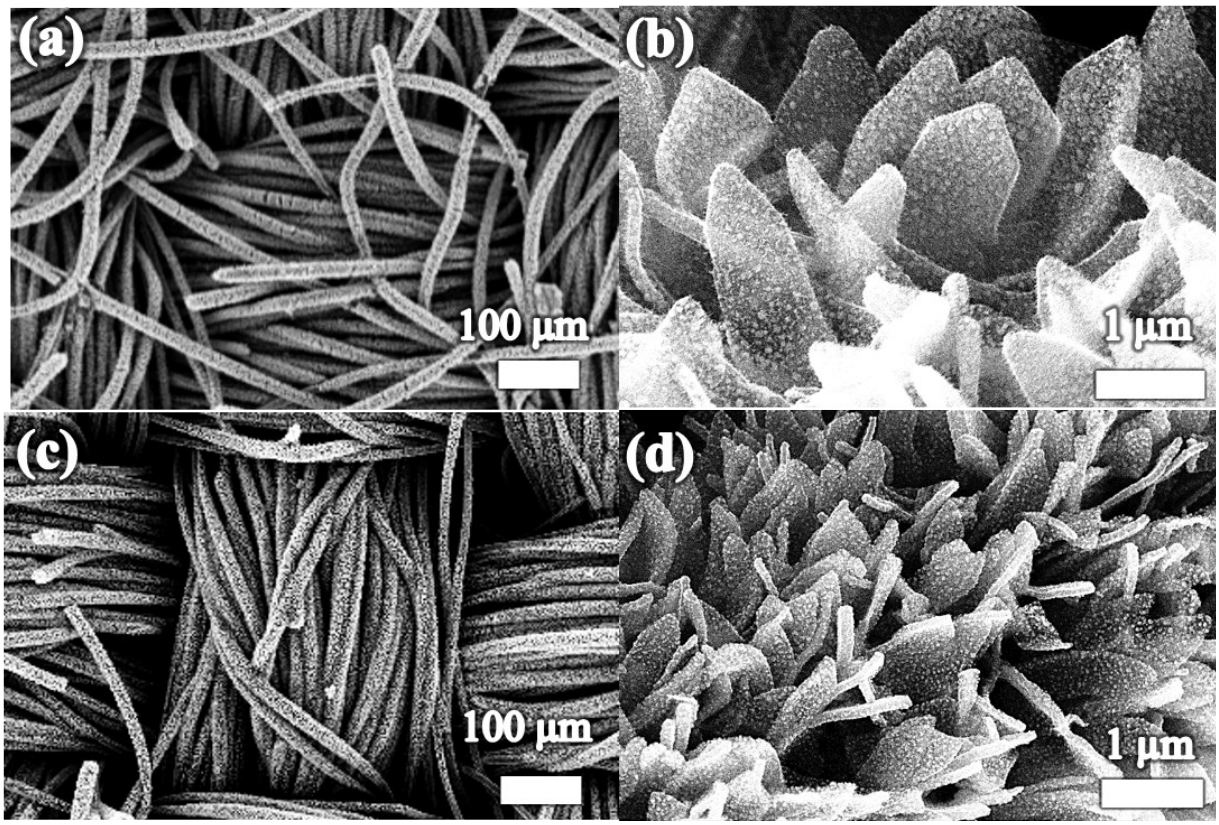

Figure S2. Additional SEM images for (a-b) NC-CNT/Co and (c-d) NC-CNT/CoP. Related to Figure 1.

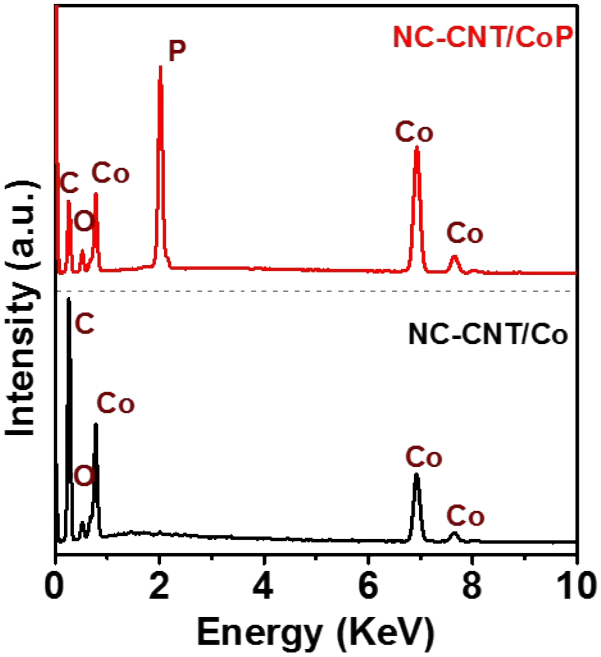

Figure S3. EDX results of NC-CNT/Co and NC-CNT/CoP. Related to Figure 1 and Figure 2.

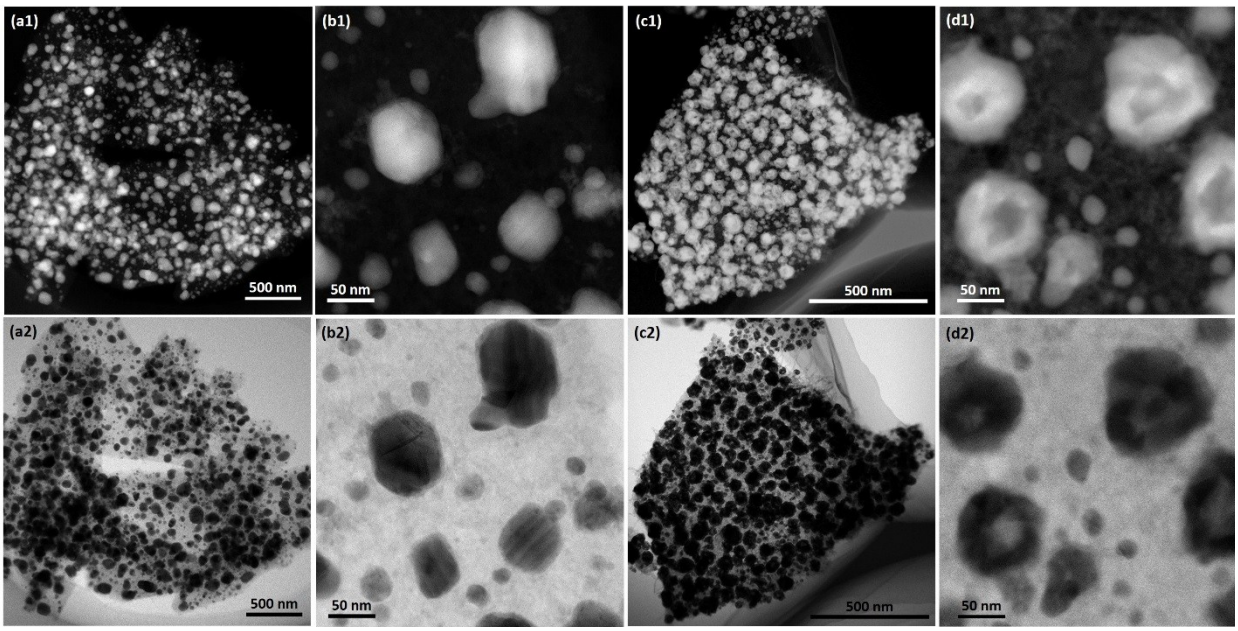

Figure S4. STEM HAADF/ABF images of NC-CNT/Co (a,b) and NC-CNT/CoP (c,d). Related to Figure 2.

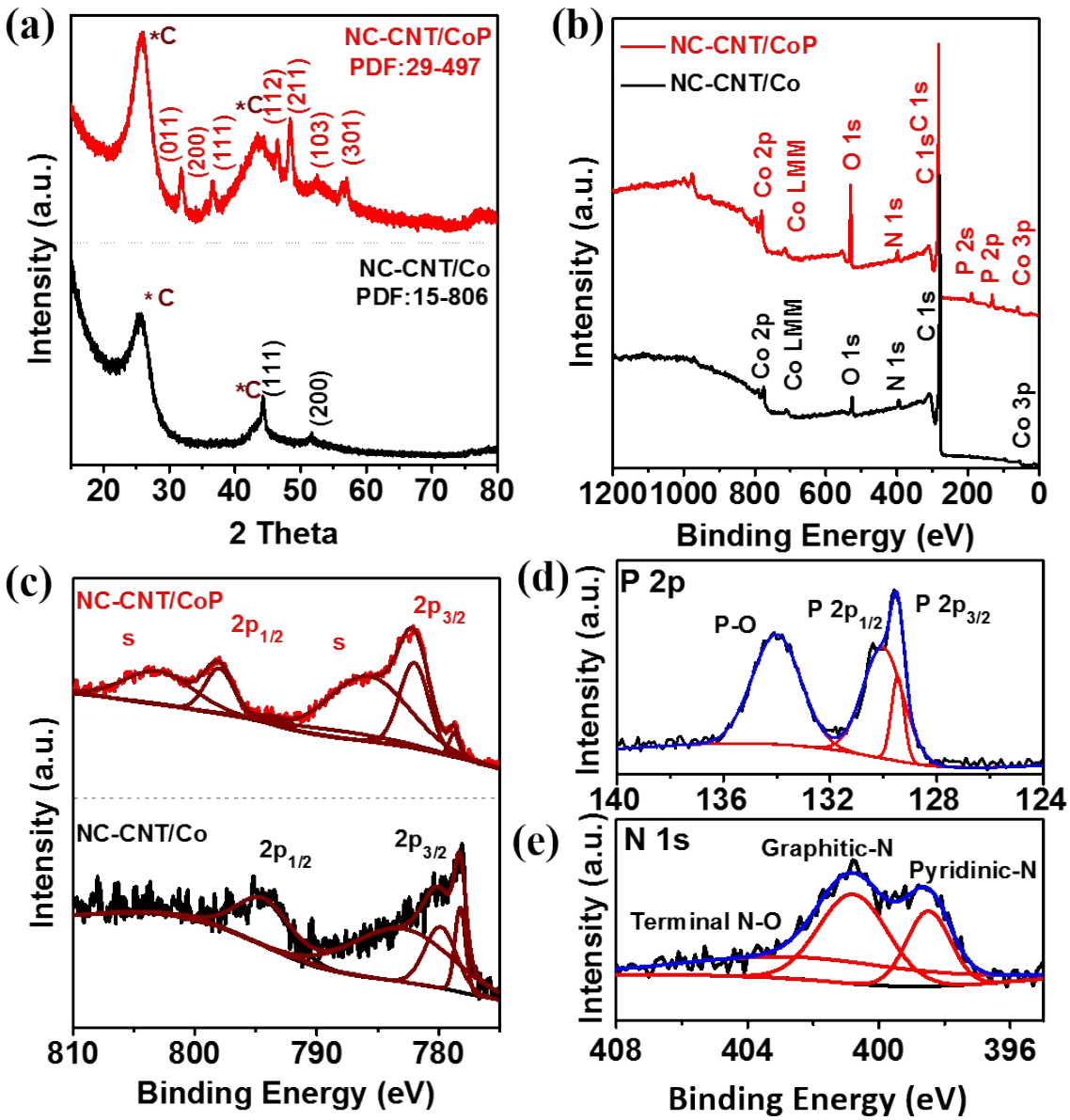

Figure S5. (a) XRD results of NC-CNT/Co and NC-CNT/CoP. (b) XPS broad scan of NC-CNT/Co and NC-CNT/CoP. (c) Co 2P spectra of NC-CNT/Co and NC-CNT/CoP. (d) P 2p spectra and (e) N 1s spectra of NC-CNT/CoP.

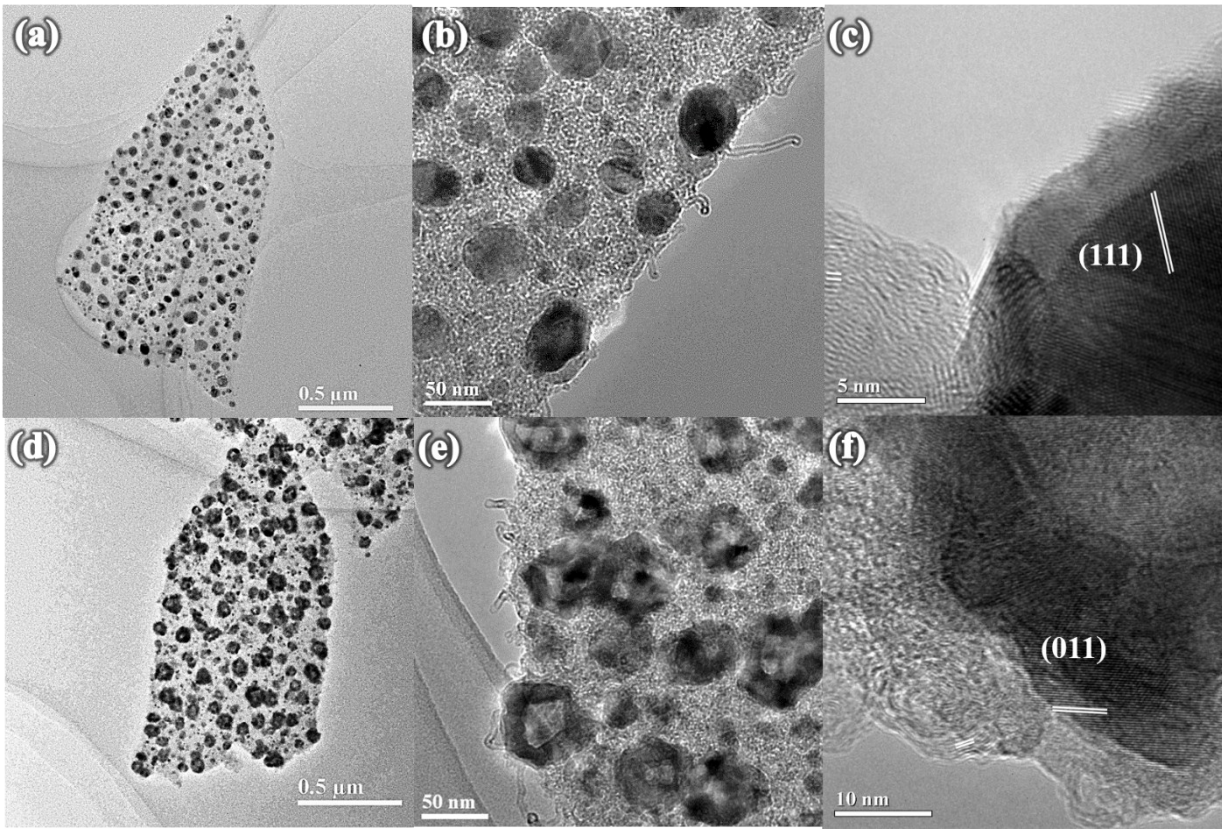

Figure S6. TEM image of (a-c) NC-CNT/Co and (d-f)NC-CNT/CoP. After reaction in Ar/H_2 (Figure S6a-b), nanoparticles with diameters of 30-50 nm are uniformly embedded in the nanowall-like carbon, while CNTs also appeared on the surface of the nanowall. Figure S6c clearly shows the nanoparticle is solid, and the lattice fringe of 0.2 nm matched well with (111) plane of Co (JCPDS card No. 15-806), indicating Co nanoparticles have been embedded in N-doped carbon-CNT nanowalls. Figure S6d-f illustrate the materials after phosphidation, from which one can see the carbon structure keeps well after the process, while the Co metal nanoparticles expand and hollow spheres formed during the reaction. Typical hollow spheres have diameters of ~60-80 nm with wall-thickness of ~10-20 nm. In Supplementary Fig. 6f, the lattice fringes of 0.28 nm corresponds well with (011) plane of CoP (JCPDS card No. 29-497). Related to Figure 2 and Figure 3.

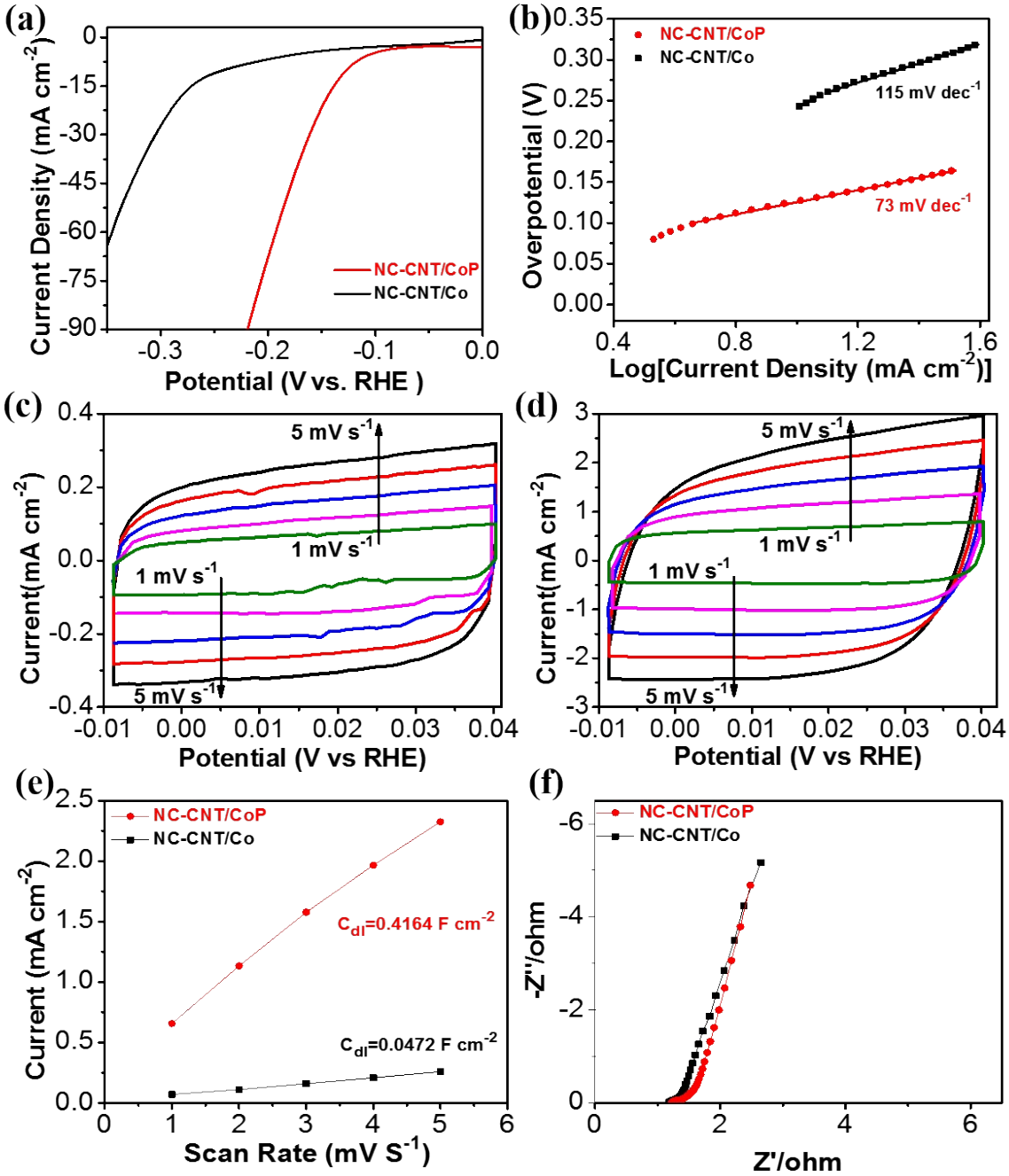

Figure S7. Comparison of electrochemical properties of NC-CNT/Co and NC-CNT/CoP. (a) Polarization curves, (b) Tafel plots results. CV curves of (c) NC-CNT/Co and (d) NC-CNT/CoP. (e) Plot of current density (@0.015 V vs RHE) vs scan rates, (f) Nyquist plots of NC-CNT/Co and NC-CNT/CoP. Related to Figure 4.

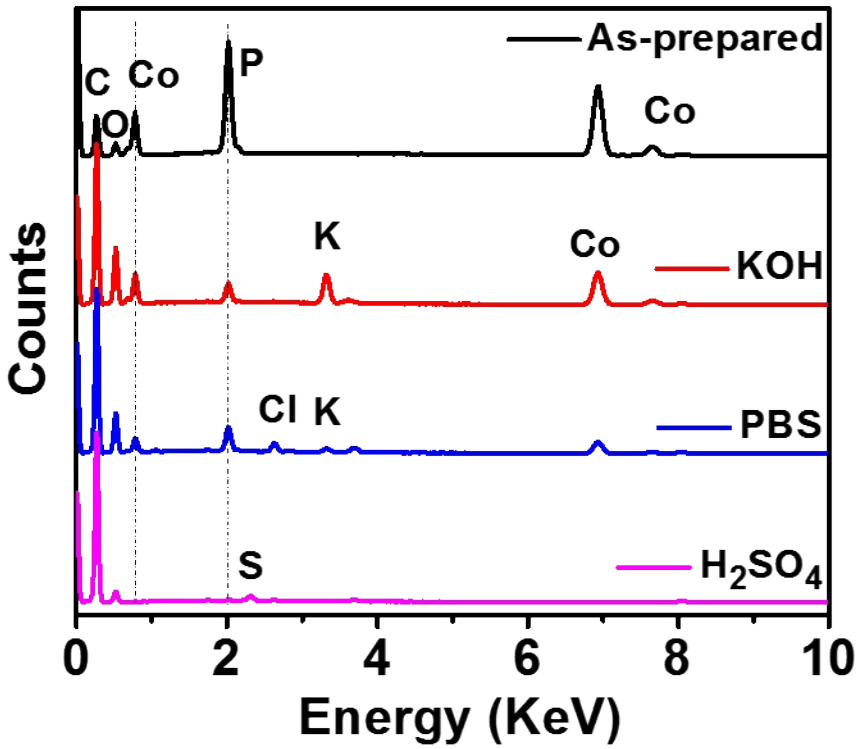

Figure S8. EDS results of the materials in situ formed after activation of NC-CNT/CoP in alkaline, neutral, and acidic electrolytes.

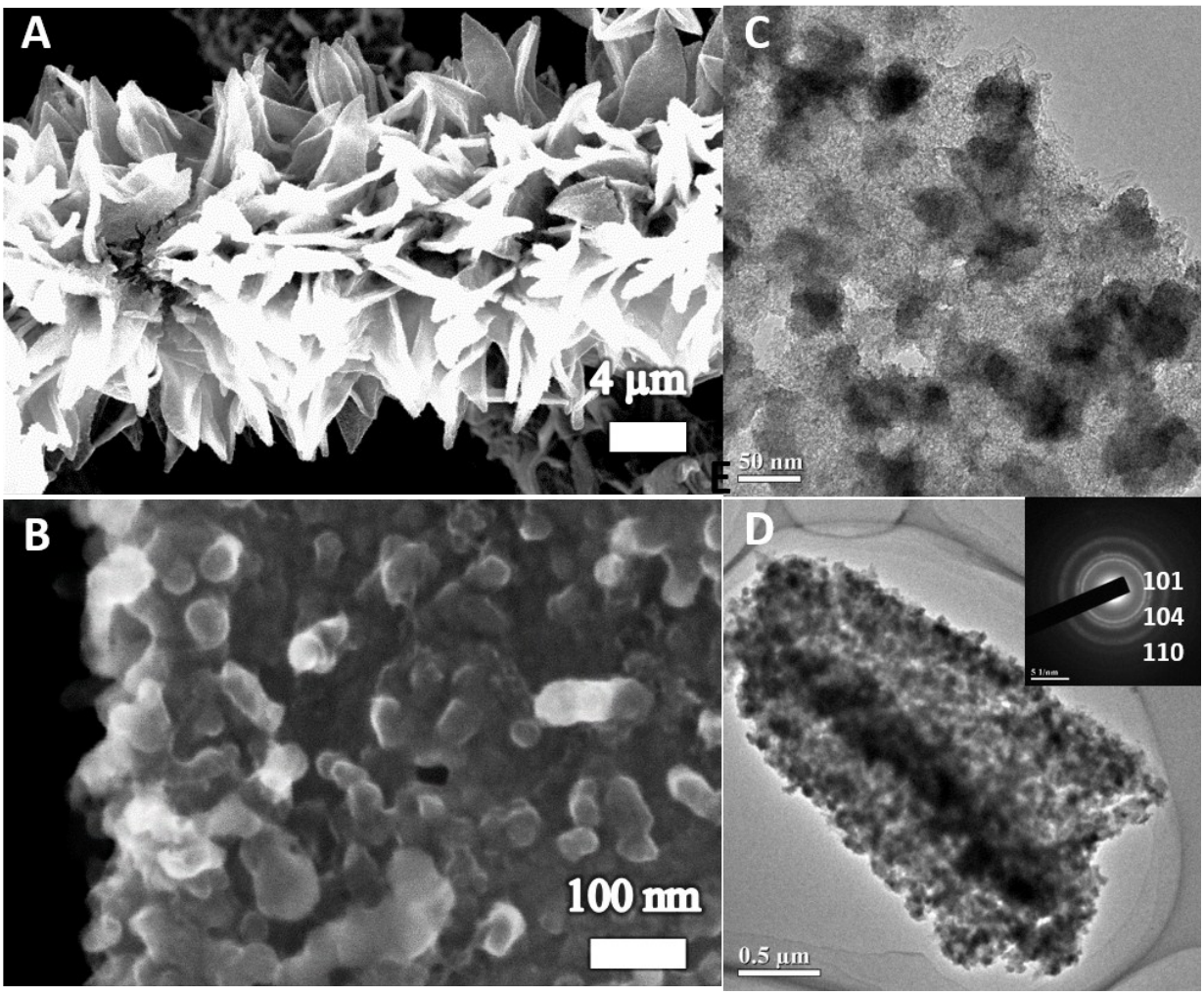

Figure S9. Characterization of the material in situ formed after activation of NC-CNT/CoP in alkaline electrolyte.

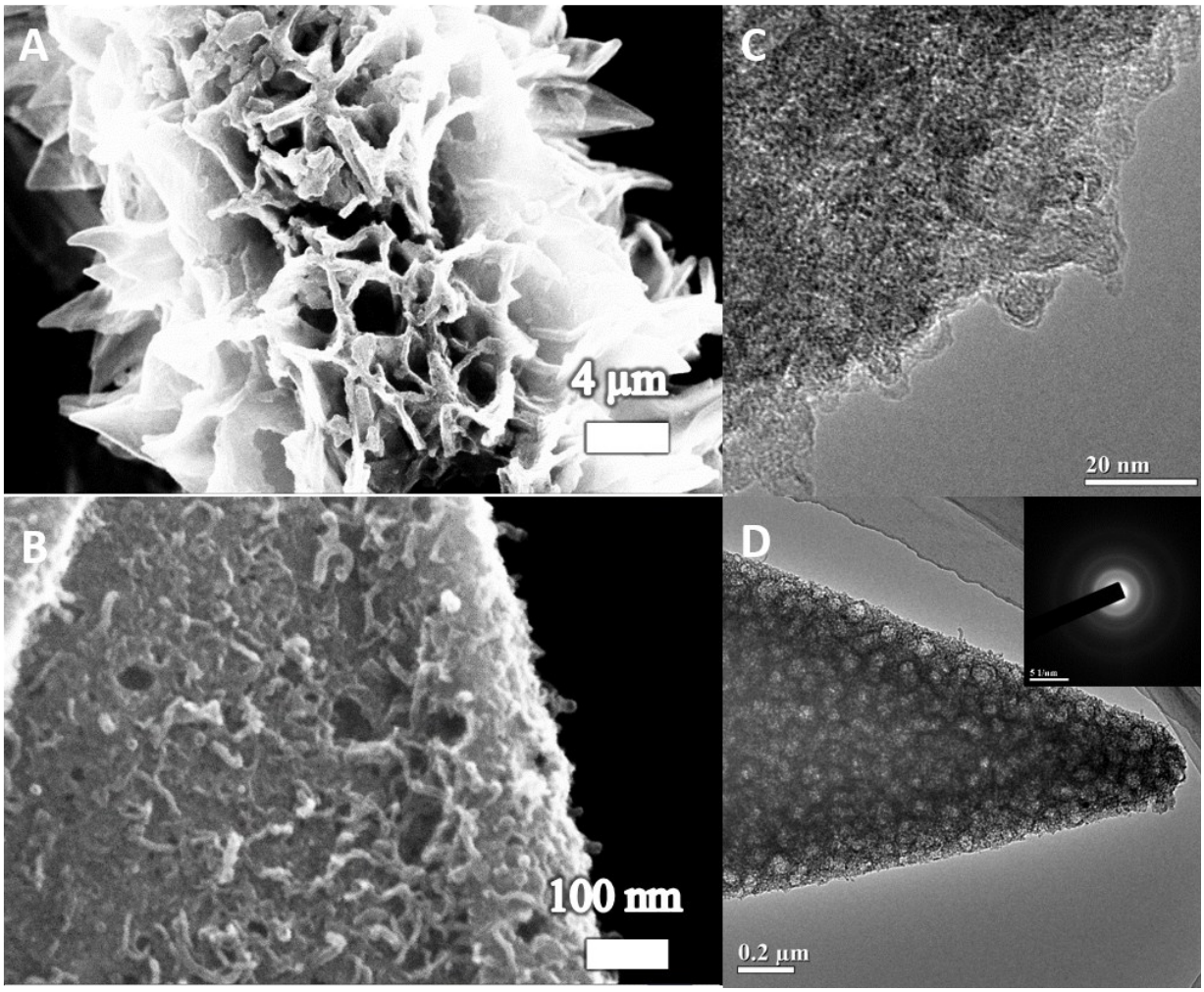

Figure S10. Characterization of the material in situ formed after activation of NC-CNT/CoP in acidic electrolyte.

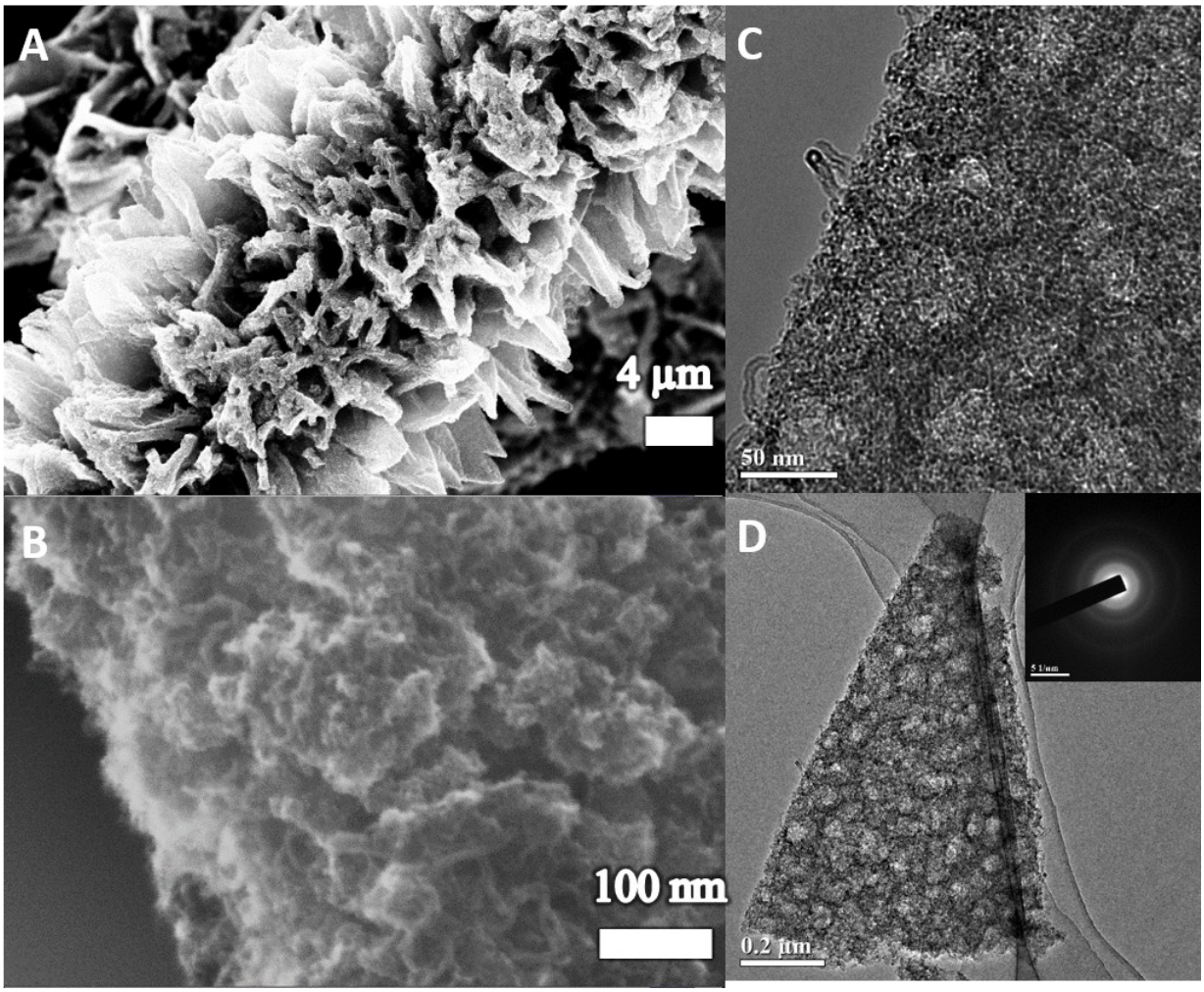

Figure S11. Characterization of the material in situ formed after activation of NC-CNT/CoP in neutral electrolyte.

Supporting Tables

Table S1. Summary of recent reported highly active **HER** catalysts in 1 M KOH electrolyte.

Catalyst	Substrate	Mass loading (mg cm^{-2})	Current density (mA cm^{-2})	Potential (V vs. RHE)	Tafel Slope (mV dec^{-1})	Reference
NC-CNT/CoP	Carbon Cloth	1.5	-10	-0.12	73	Current Work
CoPx nanoparticles embedded in N-doped carbon	GC/powder	0.283	-10	-0.145	51	[1]
$NiCo_2O_4$ Hollow Microcuboids	Ni foam/powder	1	-10	-0.110	497	[2]
Co/CoP	GC/powder	0.22	-10	-0.253	73.8	[3]
Co_9S_8@MoS_2/CNFs	GC/powder	0.212	-10	-0.19	110	[4]
Carbon tubes/ cobalt-sulfide	Carbon paper	0.32(Co-S)	-10	-0.19	131	[5]
Hollow Co3O4 Microtube Arrays	Ni foam	N.A.	-20	-0.19	98	[6]
Ni_8P_3	Ni foam	N.A.	-10	-0.13	58.5	[7]
MoS_2/Ni_3S_2	Ni foam	9.7	-10	-0.11	83	[8]
NiCoP	Ni foam	1.6	-10	-0.032	37	[9]
$Ni_{1-x}Co_xSe_2$ mesoporous nanosheet	Ni foam	2.16	-10	-0.085	52	[10]
NiFe LDH	Ni foam	N.A.	-10	-0.21	N.A.	[11]
CoN_x/C	GC/powder	2	-10	-0.17	75	[12]
Cobalt embedded nitrogen-rich carbon nanotubes	GC/powder	0.28	-10	-0.37	N.A.	[13]
FeP nanorod arrays	Carbon cloth	1.5	-10	-0.218	146	[14]
CoP nanowire arrays	Carbon Cloth	0.92	-10	-0.209	129	[15]
Ni–Mo/Cu nanowires	Cu foam	2.17	-10	-0.115	107	[16]
Cu_3P	Ni foam	0.25	-10	-0.13	83	[17]

Table S2. Summary of recent reported highly active **HER** catalysts in 0.5 M H_2SO_4 electrolyte.

Catalyst	Substrate[a, b]	Mass loading (mg cm^{-2})	Current density (mA cm^{-2})	Potential (V vs. RHE)	Tafel Slope (mV dec^{-1})	Reference
NC-CNT/CoP	Carbon Cloth	1.5	-10	-0.062	39	Current Work
$Ni_{1-x}Co_xSe_2$ mesoporous nanosheet	Ni foam	2.16	-10	-0.052	39	[10]
Cobalt phosphosulfide/CNT	carbon fibre paper/powder	1.6	-10	-0.048	55	[18]
nanoplates	GC/powder	N.A.	-10	-0.048	56	[19]
$Fe_xCo_{1-x}P$ Nanowire Array	Carbon cloth	2.2	-10	-0.037	30	[20]
Co/CoP	GC/powder	0.88	-10	-0.178	59.1	[3]
CoN_x/C	GC/powder	2	-10	-0.133	57	[12]
Cobalt embedded nitrogen-rich carbon nanotubes	GC/powder	0.28	-10	-0.26	69	[13]
FeP nanorod arrays	Carbon cloth	1.5	-10	-0.058	45	[14]
CoMoP@C	GC/powder	0.354	-10	-0.041	49.73	[21]
CoP nanowire arrays	Carbon Cloth	0.92	-10	-0.067	51	[15]

Table S3. Summary of recent reported highly active **HER** catalysts in neutral electrolyte.

Catalyst	Substrate[a, b]	Mass loading (mg cm^{-2})	Current density (mA cm^{-2})	Potential (V vs. RHE)	Tafel Slope (mV dec^{-1})	Reference
NC-CNT/CoP	Carbon Cloth	1.5	-10	-0.045	77	Current Work
$Ni_{1-x}Co_xSe_2$ mesoporous nanosheet	Ni foam	2.16	-10	-0.082	78	[10]
Co/CoP	GC/powder	0.88	-10	-0.138	72.3	[3]
CoN_x/C	GC/powder	2	-10	-0.247	N.A.	[12]
Cobalt embedded nitrogen-rich carbon nanotubes	GC/powder	0.28	-10	-0.54	N.A.	[13]
FeP nanorod arrays	Carbon cloth	1.5	-10	-0.202	71	[14]
Co-S	FTO	0.08(Co)	-10	~-0.167	93	[22]

Table S4. The results of H∗ absorbed on the CoP surface or graphene layer or nitrogen-doped graphene layer in different models. $\Delta E(H*)$, ZPE($H*$), ΔZPE, and ΔG($H*$) are the binding energy, zero point energy, zero point energy change, and adsorption free energy. While models with ' denotes adsorption sites of H∗ on carbon or nitrogen-doped carbon layer, without ' means adsorption sites of H∗ on the (200) facet of CoP with P-termination. The theorectical models and the adsorption sites are shown in Figure 5a.

models	adsorption site	$\Delta E(H^*)$/eV	ZPE(H^*)/eV	ΔZPE/eV	ΔG(H^*)/eV
NC-CoP	1	-0.160	0.217	0.080	0.125
	2	-0.218	0.217	0.080	0.066
	3	-0.462	0.219	0.082	-0.175
	4	-0.494	0.219	0.082	-0.207
C-CoP	2	-0.536	0.214	0.077	-0.254
	4	-0.684	0.219	0.081	-0.398
CoP	2	-0.580	0.214	0.076	-0.299
	4	-0.697	0.221	0.083	-0.409
NC-CoP'	5	0.863	0.309	0.172	1.241
	6	1.302	0.303	0.165	1.673
	7	2.137	0.337	0.199	2.542
C-CoP'	5	1.193	0.287	0.149	1.547
	6	1.160	0.289	0.151	1.517
	7	1.120	0.288	0.151	1.476

Theoretical models

The (200) facet with P-termination is adopted to act as the active surface for the CoP according to experiments as well as theoretical comparisons between P-termination and Co-termination, which is modeled by the slab with three layers of Co-P atoms along (200) direction and 3 × 3 supercell in the plane perpendicular to (200) direction. The convergence of dependence on number of layers was carefully checked and 3 × 3 supercell is the minimum size which gives negligible mismatch of lattice constants between CoP and graphene supercells. When sole CoP is considered, there are 108 atoms in total with half Co and half P, while in the case of CoP covered by graphene, we have additional64 carbon atoms. We sampled the nitrogen-doped graphene layer with the ratio of 1 : 7 between nitrogen and carbon atoms. We only consider the most favorable configuration in energy. The lattice constant of the slab are 9.84 Å, 16.90 Å, 26.621 Å. The two lower layer of CoP are fixed and the top layer together with graphene or nitrogen-doped graphene layer and hydrogen atom are allowed to relax. Fig. 2 shows the theoretical model for CoP covered by nitrogen-doped graphene. The models for CoP covered by graphene and CoP can be simply obtained by replacing all the nitrogen atoms by carbon atoms and removing the nitrogen-doped graphene layer, respectively.

Free energy calculation

The stability of hydrogen can be described by the free energy of adsorbed atomic hydrogen,

which is defined as

$$\Delta G(H^*) = \Delta E(H^*) + \Delta \mathrm{ZPE}(H^*) - T\Delta S(H^*) \qquad (1)$$

with

$$\Delta E(H^*) = E_{\mathrm{slab+H}} - (E_{\mathrm{slab}} + \frac{1}{2}H_2) \qquad (2)$$

where $E_{\mathrm{slab+H}}$ is the total energy for system with hydrogen atom adsorbed on the surface, E_{slab} is the total energy for systems without hydrogen atom, H_2 is the energy for a molecule in gas phase. $\Delta E(H^*)$, $\Delta \mathrm{ZPE}(H^*)$, and $\Delta S(H^*)$ denote the binding energy, zero point energy change and entropy change of H* adsorption, respectively. Here, the $\Delta S(H^*)$ can be obtained from equation： $\Delta S(H^*) = S(H^*) - \frac{1}{2}S(H_2)$, where the contribution from configuration entropy in the adsorbed state is small and is neglected. Thus we can easily conclude that the corresponding $T\Delta S(H^*)$ is ~0.205meV since $TS(H_2)$ is 0.41eV for H_2 at 300K and 1atm.

Table S5. Summary of recent reported highly active **OER** catalysts in 1 M KOH or NaOH electrolyte.

Catalyst	Substrate	Mass loading (mg cm^{-2})	Current density (mA cm^{-2})	Potential (V vs. RHE)	Tafel Slope (mV dec^{-1})	Reference
NC-CNT/CoOOH	Carbon Cloth	1.5	10	1.47	76	Current Work
N-doped carbon nanotube frameworks	Glassy carbon (GC)/powder	0.2	10	1.60	93	[23]
CoPx nanoparticles embedded in N-doped carbon	GC/powder	0.283	10	1.549	52	[1]
CoMnP nanoparticles	GC/powder	0.284	10	1.56	61	[24]
Cobalt-based borate nanosheets/ graphene	GC/powder	0.285	10	1.52	53	[25]
$Co_3O_4/NiCo_2O_4$ double-shelled nanocages	Ni foam/powder	1	10	1.57	88	[26]
$NiCo_2O_4$ Hollow Microcuboids	Ni foam/powder	1	10	1.52	53	[2]
Surface Oxidized CoP Nanorods	GC/powder	0.71	10	1.55	71	[27]
Co/CoP	GC/powder	0.22	10	1.57	79.5	[3]
NiCo LDH nanosheets	carbon paper	0.17	10	1.597	40	[28]
Co_3O_4-Carbon Nanowire Arrays	Cu foil	0.2	10	1.52	70	[29]
Hollow Co_3O_4 Microtube Arrays	Ni foam	N.A.	150	1.59	84	[6]
Carbon tubes/ cobalt-sulfide	Carbon paper	0.32 (Co-S)	10	1.536	72	[5]
Ni_8P_3	Ni foam	N.A.	30	1.5	73.2	[7]
MoS_2/Ni_3S_2	Ni foam	9.7	10	1.448	88	[8]
NiCoP	Ni foam	1.6	10	1.51	87	[9]
NiFe LDH	Ni foam	N.A.	10	1.47	N.A.	[11]
$Co_9S_8@MoS_2$/CNFs	Glassy carbon (GC)/powder	0.212	10	1.66	61	[4]
NiCoP/C	GC/powder	0.05	10	1.56	96	[30]
Ni–Mo/Cu nanowires	Cu foam	2.17	20	1.51	66	[16]

Table S6. Summary of recent reported highly active **OER** catalysts in neutral electrolyte.

Catalyst	Substrate[a, b]	Mass loading (mg cm^{-2})	Current density (mA cm^{-2})	Potential (V vs. RHE)	Reference
NC-CNT/CoP-N	Carbon Cloth	1.5	10	1.65	Current Work
Cobalt-based borate nanosheets/ graphene	GC/powder	0.285	14.4	1.8	[25]
Co/CoP	GC/powder	0.88	2.64	1.8	[3]
Co_3S_4 nanosheets	GC/powder	0.28	3.27	1.88	[31]
$Co(PO_3)_2$	Ni foam	1.1	7.1	1.67	[32]
$LiCoPO_4$	GC/powder	0.1	0.5	1.8	[33]
Co_3O_4/SWCNT	ITO/powder	0.05	6	1.8	[34]

Table S7. Summary of recent reported representative of highly active catalysts for overall water-splitting

Catalyst	Substrate	Mass loading (mg cm^{-2})	Current density (mA cm^{-2})	Voltage	Electrolyte	Reference
NC-CNT/CoP //NC-CNT/CoOOH	Carbon Cloth	1.5	10	1.63	1 M KOH	Current Work
NC-CNT/CoP //NC-CNT/CoP-N	Carbon Cloth	1.5	10	1.69	1 M PBS	
NC-CNT/CoP //NC-CNT/CoP-A	Carbon Cloth	1.5	10	1.66	0.5 M H_2SO_4	
Surface Oxidized CoP Nanorods	titanium felt sheet/powder	5	10	1.587	1 M KOH	[27]
$NiCo_2O_4$ Hollow Microcuboids	Ni foam/powder	1	10	1.65	1 M NaOH	[2]
Hollow Co_3O_4 Microtube Arrays	Ni foam	N.A.	10	1.63	1 M KOH	[6]
Carbon tubes/ cobalt-sulfide	Carbon paper	0.32(Co-S)	10	1.743	1 M KOH	[5]
Ni_8P_3	Ni foam	N.A.	10	1.61	1 M KOH	[7]
MoS_2/Ni_3S_2	Ni foam	9.7	10	1.56	1 M KOH	[8]
NiCoP	Ni foam	1.6	10	1.58	1 M KOH	[9]
NiFe LDH	Ni foam	N.A.	10	1.7	1 M NaOH	[11]
Co/CoP	GC/powder	5	10	1.45	1 M KOH	[3]
			10	1.51	1 M PBS	
			1	1.89	0.5 M H_2SO_4	
Ni–Mo/Cu nanowires	Cu foam	2.17	10	1.61	1 M KOH	[16]

Supporting references

[1] B. You, N. Jiang, M. Sheng, S. Gul, J. Yano, Y. Sun, *Chem. Mater.* **2015**, 27, 7636.
[2] X. Gao, H. Zhang, Q. Li, X. Yu, Z. Hong, X. Zhang, C. Liang, Z. Lin, *Angew. Chem. Int. Ed.* **2016**, 55, 6290.
[3] Z.-H. Xue, H. Su, Q.-Y. Yu, B. Zhang, H.-H. Wang, X.-H. Li, J.-S. Chen, *Adv. Energy Mater.* **2017**, 7, 1602355.
[4] H. Zhu, J. Zhang, R. Yanzhang, M. Du, Q. Wang, G. Gao, J. Wu, G. Wu, M. Zhang, B. Liu, J. Yao, X. Zhang, *Adv. Mater.* **2015**, 27, 4752.
[5] J. Wang, H.-x. Zhong, Z.-l. Wang, F.-l. Meng, X.-b. Zhang, *ACS Nano* **2016**, 10, 2342.
[6] Y. P. Zhu, T. Y. Ma, M. Jaroniec, S. Z. Qiao, *Angew. Chem. Int. Ed.* **2016**, 56, 1324.
[7] G.-F. Chen, T. Y. Ma, Z.-Q. Liu, N. Li, Y.-Z. Su, K. Davey, S.-Z. Qiao, *Advanced Functional Materials* **2016**, 26, 3314.
[8] J. Zhang, T. Wang, D. Pohl, B. Rellinghaus, R. Dong, S. Liu, X. Zhuang, X. Feng, *Angew. Chem.* **2016**, 128, 6814.
[9] H. Liang, A. N. Gandi, D. H. Anjum, X. Wang, U. Schwingenschlögl, H. N. Alshareef, *Nano Letters* **2016**, 16, 7718.
[10] B. Liu, Y.-F. Zhao, H.-Q. Peng, Z.-Y. Zhang, C.-K. Sit, M.-F. Yuen, T.-R. Zhang, C.-S. Lee, W.-J. Zhang, *Adv. Mater.* **2017**, n/a.
[11] J. Luo, J.-H. Im, M. T. Mayer, M. Schreier, M. K. Nazeeruddin, N.-G. Park, S. D. Tilley, H. J. Fan, M. Grätzel, *Science* **2014**, 345, 1593.
[12] H.-W. Liang, S. Brüller, R. Dong, J. Zhang, X. Feng, K. Müllen, *Nat. Commun.* **2015**, 6, 7992.
[13] X. Zou, X. Huang, A. Goswami, R. Silva, B. R. Sathe, E. Mikmeková, T. Asefa, *Angew. Chem. Int. Ed.* **2014**, 53, 4372.
[14] Y. Liang, Q. Liu, A. M. Asiri, X. Sun, Y. Luo, *ACS Catalysis* **2014**, 4, 4065.
[15] J. Tian, Q. Liu, A. M. Asiri, X. Sun, *J. Am. Chem. Soc.* **2014**, 136, 7587.
[16] S. Zhao, J. Huang, Y. Liu, J. Shen, H. Wang, X. Yang, Y. Zhu, C. Li, *Journal of Materials Chemistry A* **2017**, 5, 4207.
[17] J. Hao, W. Yang, Z. Huang, C. Zhang, *Adv. Materi. Inter.* **2016**, 3, 1600236.
[18] W. Liu, E. Hu, H. Jiang, Y. Xiang, Z. Weng, M. Li, Q. Fan, X. Yu, E. I. Altman, H. Wang, *Nat. Commun.* **2016**, 7, 10771.
[19] M. Caban-Acevedo, M. L. Stone, J. R. Schmidt, J. G. Thomas, Q. Ding, H.-C. Chang, M.-L. Tsai, J.-H. He, S. Jin, *Nat Mater* **2015**, 14, 1245.
[20] C. Tang, L. Gan, R. Zhang, W. Lu, X. Jiang, A. M. Asiri, X. Sun, J. Wang, L. Chen, *Nano Letters* **2016**.
[21] Y.-Y. Ma, C.-X. Wu, X.-J. Feng, H.-Q. Tan, L.-K. Yan, Y. Liu, Z.-H. Kang, E.-B. Wang, Y.-G. Li, *Energy Environ.Sci.* **2017**, 10, 788.
[22] Y. Sun, C. Liu, D. C. Grauer, J. Yano, J. R. Long, P. Yang, C. J. Chang, *J. Am. Chem. Soc.* **2013**, 135, 17699.
[23] L. Jiao, Y.-X. Zhou, H.-L. Jiang, *Chem. Sci.* **2016**, 7, 1690.
[24] D. Li, H. Baydoun, C. N. Verani, S. L. Brock, *J. Am. Chem. Soc.* **2016**, 138, 4006.
[25] P. Chen, K. Xu, T. Zhou, Y. Tong, J. Wu, H. Cheng, X. Lu, H. Ding, C. Wu, Y. Xie, *Angew. Chem. Int. Ed.* **2016**, 55, 2488.
[26] Z.-H. Huang, Y. Song, X.-X. Xu, X.-X. Liu, *ACS Applied Materials & Interfaces* **2015**, 7, 25506.
[27] J. Chang, Y. Xiao, M. Xiao, J. Ge, C. Liu, W. Xing, *ACS Catalysis* **2015**, 5, 6874.
[28] H. Liang, F. Meng, M. Cabán-Acevedo, L. Li, A. Forticaux, L. Xiu, Z. Wang, S. Jin, *Nano Letters* **2015**, 15, 1421.
[29] T. Y. Ma, S. Dai, M. Jaroniec, S. Z. Qiao, *J. Am. Chem. Soc.* **2014**, 136, 13925.
[30] P. He, X.-Y. Yu, X. W. Lou, *Angew. Chem. Int. Ed.* **2017**, 56, 3897.
[31] Y. Liu, C. Xiao, M. Lyu, Y. Lin, W. Cai, P. Huang, W. Tong, Y. Zou, Y. Xie, *Angew. Chem. Int. Ed.* **2015**, 54, 11231.

[32] H. S. Ahn, T. D. Tilley, *Advanced Functional Materials* **2013**, 23, 227.
[33] S. W. Lee, C. Carlton, M. Risch, Y. Surendranath, S. Chen, S. Furutsuki, A. Yamada, D. G. Nocera, Y. Shao-Horn, *J. Am. Chem. Soc.* **2012**, 134, 16959.
[34] J. Wu, Y. Xue, X. Yan, W. Yan, Q. Cheng, Y. Xie, *Nano Research* **2012**, 5, 521.